Publié dans Inorganica Chimica Acta 357, issue 7, 2007-2014, 2004
qui doit être utilisé pour toute référence à ce travail

Protonation and Zn(II) complexation with versatile valine and glycylglycine *N*-pyrimidines derivatives: crystal structures of layered $\{[Zn(HL1)_2]\cdot 2H_2O\}_n$ and $[Zn(HL2)_2(H_2O)_4]$

R. López-Garzón [a,*], M.L. Godino-Salido [a], P. Arranz-Mascarós [a], M.A. Fontecha-Cámara [a], M.D. Gutiérrez-Valero [a], R. Cuesta [a,*], J.M. Moreno [b], H. Stoeckli-Evans [c]

[a] *Department of Inorganic and Organic Chemistry, University of Jaén, 23071 Jaén, Spain*
[b] *Department of Inorganic Chemistry, University of Granada, 18071 Granada, Spain*
[c] *Institute of Chemistry, University of Neuchâtel, CH-2007 Neuchâtel, Switzerland*

Abstract

Protonation and Zn(II) complexation of N-substituted amino acids, valine (H_2**L1**) and glycylglycine (H_2**L2**), with 4-amino-1,6-dihydro-1-methyl-5-nitroso-6-oxopyrimidin-2-yl as substituent, were studied by potentiometric and UV–Vis measurements. Bianions **L1** and **L2** suffer three protonation steps in aqueous medium corresponding to the amide and carboxylate groups of the amino acidic moiety, and the nitrogen atom of the nitroso group of the pyrimidine fragment. Both ligands form mononuclear Zn(II) complexes in aqueous solutions. The binding donor groups are the nitroso and/or the oxo groups of the pyrimidinic moiety or the carboxylate group, depending on whether the ligands are neutral or anionic, respectively. Weak metal-to-ligand interactions were observed independently of the functionality used by the corresponding ligand on bonding to Zn(II). The reaction of $ZnCl_2$ with the monodeprotonated ligands (1:1) yields a polynuclear 2D $\{[Zn(HL1)_2]\cdot 2H_2O\}_n$ and a mononuclear $[Zn(HL2)_2(H_2O)_4]$ complexes, showing the influence of the susbtituent on the amino acids fragment as well as the versatility of this class of compounds when acting as ligands.

Keywords: Crystal structures; Zinc complexes; Titrations

1. Introduction

N-substituted α-amino acids with 4-amino-1,6-dihydro-1-methyl-5-nitroso-6-oxopyrimidin-2-yl as substituent are molecular compounds consisting of a pyrimidinic rigid moiety with an amino acidic pendant moiety. These compounds are potential ligands against metal ions, having as potential donor groups the amino acidic moiety (including the carboxylate anion and the potential donor atoms of the R substituent existing on Cα) and C5NO and C6O groups of the pyrimidinic moiety. This, together with the rigidity of the pyrimidinic moiety, favours the formation of 1D, 2D and 3D polynuclear solid complexes whose crystal structures feature, in some cases, those of metal–organic compounds with non-linear optic properties [1].

In this paper, the crystal structure of H_2**L2** is compared to H_2**L1** one and those of other analogous ligands [2,3]. The acidic/base behaviour of both of the compounds and their reactivities with Zn(II) in aqueous medium are discussed and the crystal and molecular structures of $\{[Zn(HL1)_2]\cdot 2H_2O\}_n$ (**1**) (polynuclear 2D) and $[Zn(HL2)_2(H_2O)_4]$ (**2**) (mononuclear) complexes, are also reported.

* Corresponding authors. Tel.: +953026568; fax: +953026508.
E-mail addresses: rlopez@ujaen.es (R. López-Garzón), rmcuesta@ujaen.es (R. Cuesta).

2. Results and discussion

2.1. Ligands protonation

The protonation equilibria of the ligands have been studied by potentiometric measurements in solution (0.1 mol dm^{-3} KCl, 298.1 K) and the results are reported in Table 1. The $HL1^-$ species binds two protons in the pH range 2.5–10. A third protonation step of $L1^{2-}$ species (log K value ca. 12.2) was monitored above pH 10 using spectrophotometric measurements.

The second and third protonation constants (Table 1) indicate low proton affinities of the donor atoms. The log K value for $HL1^- + H^+ = H_2L1$ process (3.19) is in the range expected for the protonation of carboxylate anion. The log K for $H_2L1 + H^+ = [H_3L1]^+$, 2.23, indicates a lower basicity as expected for the remaining basic positions, all of them being in the pyrimidinic moiety. The absorption spectra, recorded on solutions of H_2L1 at various pH values (Fig. 1), are similar to the pyrimidine chromophore 2,4-diamine-1,6-dihydro-1-methyl-5-nitroso-6-oxopyrimidine [4]. The protonation of the pyrimidinic moiety in H_2L1 gives rise to disappearance of an absorption band at 326.8 nm and to a new blue-shifted absorption band with λ_{max} at 275 nm. Moreover, this protonation produces the vanishing of the visible band at 525 nm which also disappears during the reaction of the analogous glycine derivative with Cu(II) at pH of ca. 2.2. In this reaction, a complex is formed with a 1:2 metal-to-ligand ratio in which the metal ion is coordinated to the nitrogen atom of C5–NO group [5]. Thus, the blocking of the σ electronic pair seems to produce the disappearance of the absorption band, suggesting a protonation or metallation of C5–NO group. The protonation of NO group instead of N3 cyclic atom in the pyrimidinic moiety is consistent with the bipolar nature of H_2L1 molecule (Scheme 1) and implies the location of a negative charge on the former group and a positive one on the latter [2].

Fig. 1(a) shows the spectral changes occurring in the UV–Vis absorption spectra under this protonation step, starting two pH units above log K_a [6], as expected. In addition to this, UV–Vis technique (Fig. 1(b)) reveals the existence of a third protonation process on $L1^{2-}$ (log K value ca. 12.2) which was not detected by potentiometry, affecting one of the previously deprotonated groups attached to the C2 and C4 atoms of the pyrimidinic moiety. Moreover, ^{13}C NMR spectra of aqueous-solutions of H_2L1 at pH values of 6 and 12.3 point out that this process markedly affects the chemical shift of the signals of C_α, $CH_{isopropyl}$ and C_{COO}, suggesting that the proton interacts with the negatively charged N atom of the valine residue.

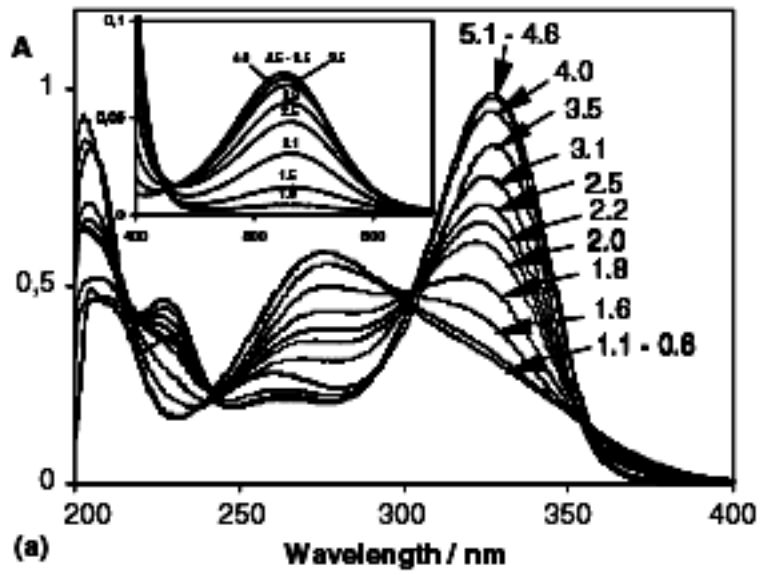

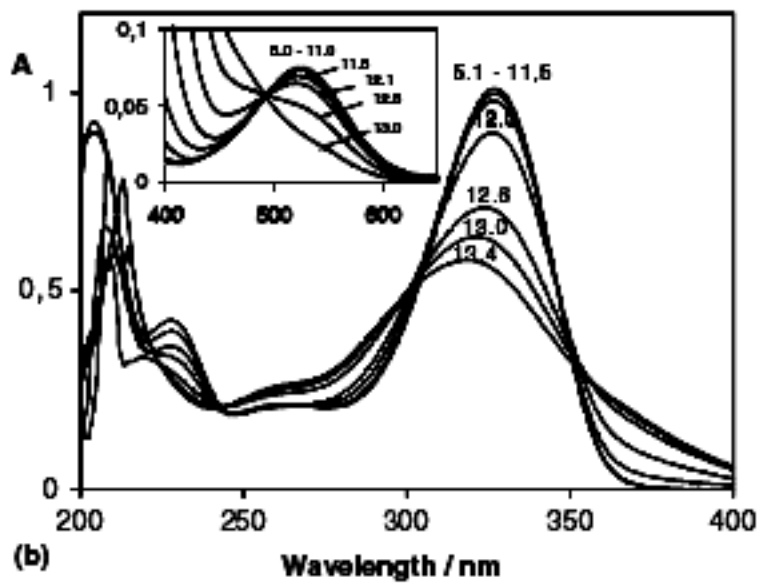

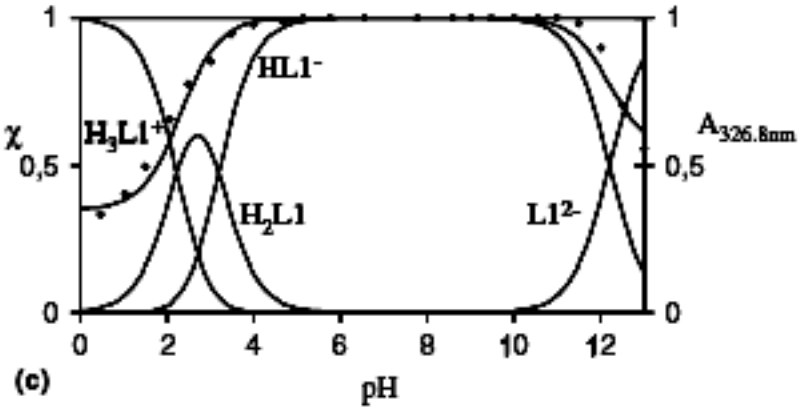

Fig. 1. (a) pH dependence of the absorption spectra in acidic media of H_2L1 in the UV ($[H_2L1] = 5\times10^{-5}$ M, $I = 0.1$ M) Inset: Ibd. In the visible ($[H_2L1] = 10^{-3}$ M, $I = 0.1$ M). (b) Ibd. In the basic media. (c) Absorbance at 326.8 nm (•) and molar fractions (χ) of the protonated form of H_2L1.

Table 1
Protonation constants (log K) of the ligands H_2L1 and H_2L2 (0.1 mol dm^{-3} KCl, 298.1 K)

Reaction	log K[a]	
	H_2L1	H_2L2
$L^{2-} + H^+ = [HL]^-$	12.2(2)	10.39(1)
$[HL]^- + H^+ = [H_2L]$	3.19(1)	3.61(2)
$[H_2L] + H^+ = [H_3L]^+$	2.23(4)	2.02(2)

[a] Values in parentheses are standard deviations on the last significant figure.

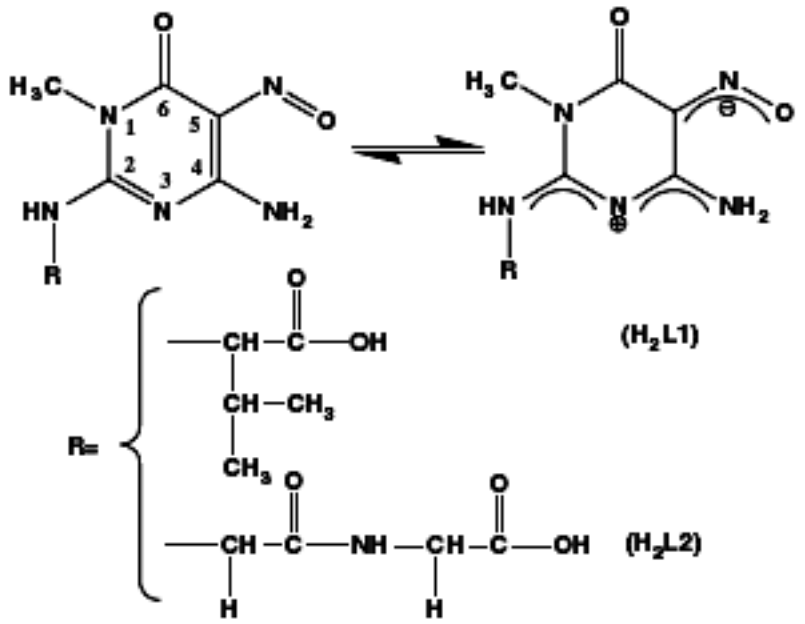

Scheme 1.

As expected, a rather like behaviour of H_2L2 was observed in the study of this ligand. Analogous protonation processes to H_2L1 are observed in the 2.5 to ca. 12 pH range (see Table 1), giving rise to analogous UV–Vis spectral changes (Fig. 2). Figs. 2(b) and (c) show that deprotonation of C2NH group starts at a pH value of ca. 9.5, about two units lower than in H_2L1, probably due to the electron withdrawing amide group existing in the glycylglycine derivative. In fact, the different polarities in NH bonds of the aminoacidic moieties of both ligands are reflected in the chemical shift values of these groups signals in the ^1H NMR (DMSO-d_6 solvent), which are 7.68 and 8.33 ppm for H_2L1 and H_2L2, respectively.

2.2. Crystal structure of *I*

The molecular unit of $\{[Zn(HL1)_2] \cdot 2H_2O\}_n$ consists of 2D layers extended in the crystal along the *bc* plane (Fig. 3). The asymmetric unit has two different bridging HL1 anions with a head to tail relative disposition. One of the ligands bridges two metal ions in a tridentate fashion through the carboxylate group and the nitrogen of the NO group and the oxygen of the C6O, in a chelating mode. The second one acts in a bidentate fashion through the carboxylate group and the NO group, but in this case oxygen being the donor atom. Each of the Zn(II) ions is linked to four HL1 molecules resulting in a pentacoordinated environment (Table 2) with a geometry intermediate between square pyramidal (with O6B, N5B, O24B and O5A in the basal positions) and trigonal bipyramidal (with O5A and O6B in the apical positions). The versatility in the use of N and O atoms of C5NO group reflects the electronic delocalization, typical in this class of ligands [2]. It is also noteworthy that the N3 cyclic atom does not act as a donor atom, as

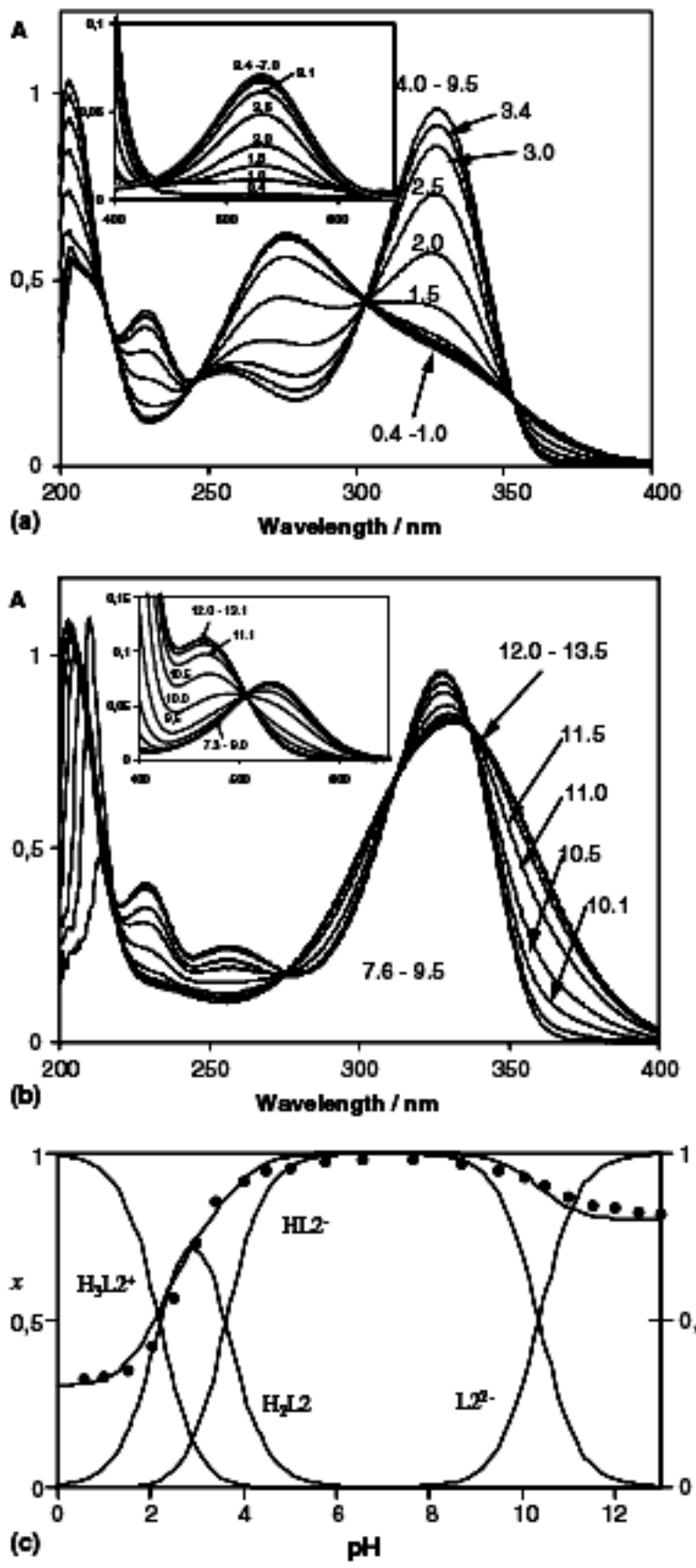

Fig. 2. (a) pH dependence of the absorption spectra in acidic media of H_2L2 in the UV ($[H_2L2]=5\times10^{-5}$ M, $I=0.1$ M) Inset: Ibd. In the visible ($[H_2L2]=10^{-3}$ M, $I=0.1$ M). (b) Ibd. In the basic media. (c) Absorbance at 327.2 nm (•) and molar fractions (χ) of the protonated form of H_2L2.

observed in several structures described for metal complexes of analogous ligands [5,7,8]. This is in agreement to the dipolar character of free H_2L1 [2], indicated by the similarity of the bond lengths in N21–C2–N3–C4–N4 and C5–N5–O5 fragments in both pyrimidinic moieties.

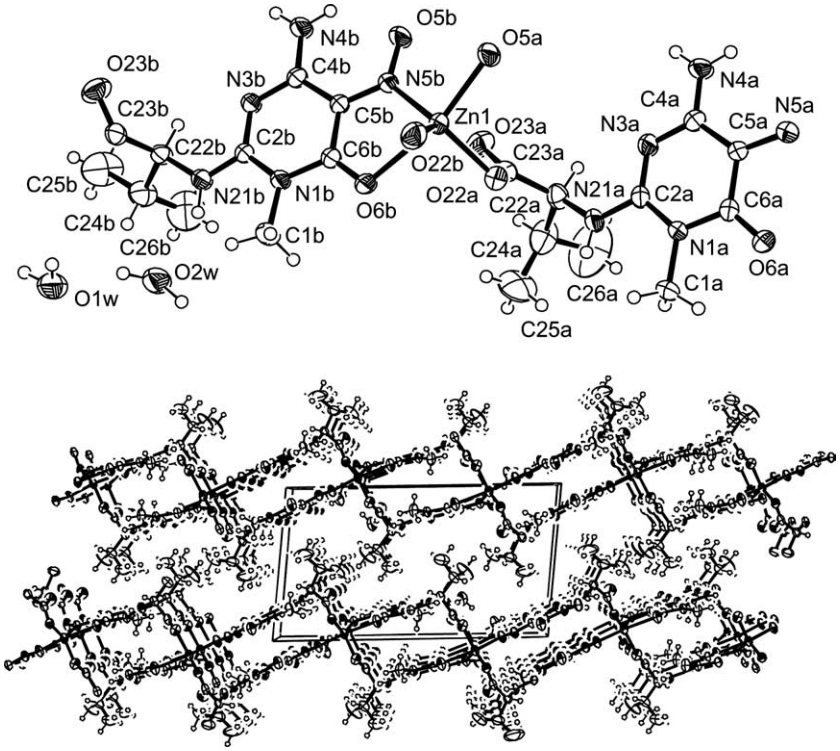

Fig. 3. (a) ORTEP drawing of the asymmetric unit and (b) packing of the molecules of $\{[Zn(H\mathbf{L1})_2]\cdot 2H_2O\}_n$.

2.3. Crystal structure of **2**

A view of the complex is shown in Fig. 4 while selected bond distances and angles are listed in Table 2, and consist of mononuclear $[Zn(H\mathbf{L2})_2(H_2O)_4]$ molecules with the Zn(II) ion coordinated by four water molecules and the two carboxylate groups of the H**L2** ligands in a *trans* position, as a result of the C_i symmetry. Thus, the planes of the pyrimidinic moieties lie parallel one to one another in such a way that the resulting structure is a regular octahedron with Zn(II) on the centre of inversion. As in **1**, bond distances in the C(5)–NO group and in the N21–C2–N3–C4–N4 fragment exhibit the changes due to the bipolar character.

In the crystal packing, the molecules of $[Zn(H\mathbf{L2})_2(H_2O)_4]$ stack with the pyrimidinic planes of symmetry related molecules parallel to one another and separated by ca. 3.9 Å. This arrangement is stabilized by a complex net of inter and intramolecular hydrogen bonds.

2.4. Zn(II) coordination in aqueous solution

Complex formation equilibria in water solutions for $H_2\mathbf{L1}$/Zn(II) and $H_2\mathbf{L2}$/Zn(II) (1:1 molar ratio) were determined from the potentiometric data obtained at 298.1 K and 0.1 mol dm^{-3} KCl ionic strength. The best fit of experimental data for $H_2\mathbf{L1}$/Zn(II) system in the pH range (2.5–7.0) corresponds to the formation equilibria of $[Zn(H_2\mathbf{L1})]^{2+}$ and $[Zn(H_2\mathbf{L1})(H\mathbf{L1})]^{+}$ complexes (Table 3). The $H_2\mathbf{L1}$ would be coordinated to Zn(II) in $[Zn(H_2\mathbf{L1})]^{2+}$ through the C5NO group. The low stability constant ($\log K = 2.48$ for $[Zn(H_2\mathbf{L1})]^{2+}$) indicates a weak interaction. It has been noted before that the donation of the σ electron pair of the nitrogen atom of NO group to a Lewis acid gives rise to the quenching of the visible absorption band of $H_2\mathbf{L1}$ at 525 nm. Thus, the existence of $[H_3\mathbf{L1}]^{+}$ species (C5NO protonated) and complex $[Zn(H_2\mathbf{L1})]^{2+}$ species in the same pH range (due to their similar stability constants, 2.23 versus 2.48) made impossible the structural characterization by analysis of visible spectrum of the $H_2\mathbf{L1}$/Zn(II) system at a different pH value. To get further insight into the nature of metal–ligand interaction in $[Zn(H_2\mathbf{L1})]^{2+}$, growing amounts of $ZnCl_2$ were added to a 10^{-3} M aqueous solution of $H_2\mathbf{L1}$ at pH 2, up to 1:10 $[H_2\mathbf{L1}]/[Zn(II)]$ ratio. Provided that no change was observed in the visible spectra and in accordance with the low $\log K$ value for this species, a NO–Zn(II) interaction seems to be probable. Fig. 5(a) shows that $[Zn(H_2\mathbf{L1})]^{2+}$ is the main complex species existing up to a pH value of ca. 2, but when $H\mathbf{L1}^{-}$ amount grows in the solution (at increasing pH values) the $[Zn(H_2\mathbf{L1})(H\mathbf{L1})]^{+}$ mixed complex emerges due to the addition of a $H\mathbf{L1}^{-}$ to an $[Zn(H_2\mathbf{L1})]^{2+}$ molecule: $[Zn(H_2\mathbf{L1})]^{2+} + H\mathbf{L1}^{-} = [Zn(H_2\mathbf{L1})(H\mathbf{L1})]^{+}$. The stability constant of $[Zn(H_2\mathbf{L1})$-

Table 2
Selected bond lengths (Å) and angles (°) for $\{[Zn(H\mathbf{L1})_2]\cdot 2H_2O\}_n$ and $[Zn(H\mathbf{L2})_2(H_2O)_4]$

$\{[Zn(H\mathbf{L1})_2]\cdot 2H_2O\}_n$			
N(3A)–C(2A)	1.317(5)	O(5A)–Zn(1)–O(6B)	165.93(10)
N(3A)–C(4A)	1.348(5)	O(5A)–Zn(1)–O(22A)	99.93(10)
N(3B)–C(2B)	1.332(4)	O(5A)–Zn(1)–N(5B)	94.96(11)
N(3B)–C(4B)	1.350(4)	O(6B)–Zn(1)–O(22A)	93.64(9)
N(4A)–C(4A)	1.302(5)	O(6B)–Zn(1)–O(22B)	82.70(11)
N(4B)–C(4B)	1.310(5)	O(6B)–Zn(1)–N(5B)	73.67(9)
N(21A)–C(2A)	1.335(4)	O(22A)–Zn(1)–N(5B)	126.97(11)
N(21B)–C(2B)	1.319(4)	O(22B)–Zn(1)–N(5B)	119.41(12)
O(22A)–C(23A)	1.275(4)		
O(22B)–C(23B)[a]	1.268(5)		
O(23A)–C(23A)	1.227(6)		
O(23B)–C(23B)	1.225(5)		
Zn(1)–O(5A)	2.087(3)		
Zn(1)–O(6B)	2.361(3)		
Zn(1)–O(22A)	1.983(3)		
Zn(1)–O(22B)	1.955(3)		
Zn(1)–N(5B)	2.085(3)		
$[Zn(H\mathbf{L2})_2(H_2O)_4]$			
N(3)–C(4)	1.344(3)	O(1W)–Zn(1)–O(2W)	94.79(9)
N(4)–C(4)	1.320(3)	O(1W)–Zn(1)–O(22)	91.59(8)
N(5)–C(5)	1.351(3)	O(1W)–Zn(1)–O(2W)[b]	85.21(9)
N(21)–C(2)	1.328(3)	O(1W)–Zn(1)–O(22)[b]	88.41(8)
N(3)–C(2)	1.325(3)	O(2W)–Zn(1)–O(22)	91.11(8)
O(22)–C(24)	1.281(3)	O(2W)–Zn(1)–O(1W)[b]	85.21(9)
O(23)–C(24)	1.222(3)	O(2W)–Zn(1)–O(22)[b]	88.89(8)
O(5)–N(5)	1.271(3)	O(22)–Zn(1)–O(1W)[b]	88.41(8)
Zn(1)–O(1W)	2.119(2)	O(22)–Zn(1)–O(2W)[b]	88.89(8)
Zn(1)–O(2W)	2.140(2)	O(1W)[b]–Zn(1)–O(2W)[b]	94.79(9)
Zn(1)–O(22)	2.055(1)	O(1W)[b]–Zn(1)–O(22)[b]	91.59(8)
		O(2W)[b]–Zn(1)–O(22)[b]	91.11(8)

[a] $2-x, -1/2+y, 1-z$.
[b] $-x-1, -y+2, -z$.

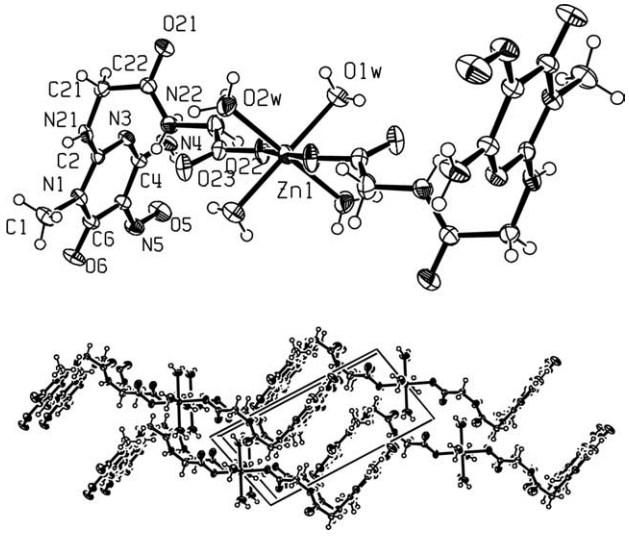

Fig. 4. (a) ORTEP drawing and (b) crystal packing of the molecules of $[Zn(H\mathbf{L2})_2(H_2O)_4]$.

$(H\mathbf{L1})]^+$ ($\log K = 2.86$), although it is slightly higher than $[Zn(H_2\mathbf{L1})]^{2+}$ species, points out the similar strength in the binding of Zn(II) to pyrimidine and

Table 3
Stability constants ($\log K$) of Zn(II) complexes with $H_2\mathbf{L1}$ and $H_2\mathbf{L2}$ (0.1 mol dm^{-3} KCl, 298.1 K)

Reaction	$\log K$[a]
$H_2\mathbf{L1} + Zn^{2+} = [Zn(H_2\ \mathbf{L1})]^{2+}$	2.48(3)
$[Zn(H_2\mathbf{L1})]^{2+} + H\mathbf{L1}^- = [Zn(H^2\mathbf{L1})(H\mathbf{L1})]^+$	2.86(8)
$2H\mathbf{L2}^- + Zn^{2+} = [Zn(H\mathbf{L2})_2]$	6.29(3)
$Zn^{2+} + H\mathbf{L2}^- + \mathbf{L2}^{2-} = [Zn(H\mathbf{L2})(\mathbf{L2})]^-$	12.63(2)

[a] Values in parentheses are standard deviations on the last significant figure.

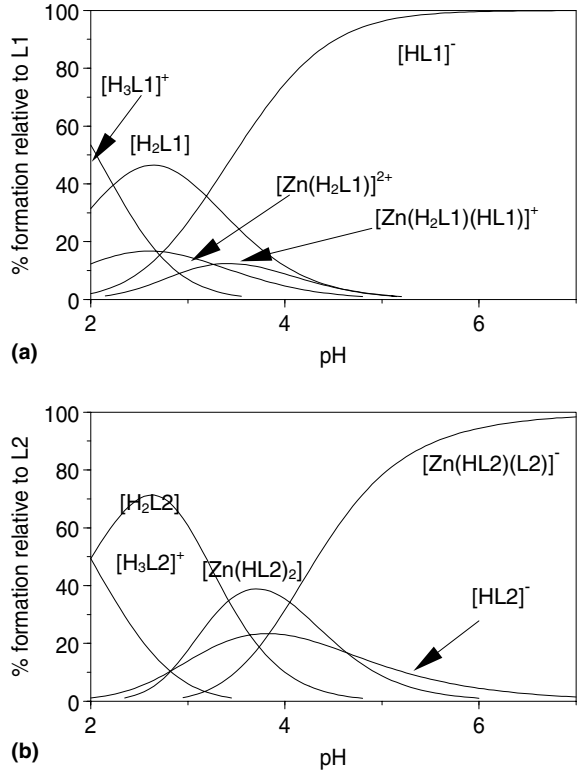

Fig. 5. Distribution species diagram as a function of pH for: (a) system $H_2\mathbf{L1}$/Zn(II) (molar ratio 1:1) and (b) system $H_2\mathbf{L2}$/Zn(II) (molar ratio 1:1).

carboxylate moieties. This would explain the trend of the mononuclear complexes existing in solution to yield the neutral polynuclear complexes with $Zn(H\mathbf{L1})_2$ stoichiometry described above; although the weakness of Zn(II)–pyrimidine interaction is also consistent with the formation of mononuclear complexes of Zn(II) with some of these types of ligands [8], embodying $[Zn(H\mathbf{L2})_2(H_2O)_4]$ complex described above.

In the $H_2\mathbf{L2}$/Zn(II) system, the unique complex existing up to pH value of 3 is the mononuclear neutral $Zn(H\mathbf{L2})_2$ species which contains two organic ligands in monoanionic form. The stability constant ($\log K = 6.29$) also reflects a weak Zn(II)–carboxylate interaction, as observed in the case of $H_2\mathbf{L1}$ ligand. At pH values higher than ca. 3, the $[Zn(H\mathbf{L2})(\mathbf{L2})]^-$ anionic mixed complex is formed by the process: $Zn(H\mathbf{L2})_2 + OH^- =$ $[Zn(H\mathbf{L2})$

(**L2**)]$^-$ + H_2O. In [Zn(H**L2**)(**L2**)]$^-$, **L2** is a bianionic ligand formed by deprotonation of NH group attached to C2 atom of the pyrimidinic moiety, which suggests the strong polarization of N–H bond induced by the metal carboxylate interaction existing in Zn(H**L2**)$_2$ species, in such a way that at a pH value of ca. 6, [Zn(H**L2**)(**L2**)]$^-$ is the unique species existing in solution.

2.5. Concluding remarks

The protonic affinities of the two nitroso-pyrimidine N-containing amino acids fit well with a polar electronic pattern for the pyrimidinic moiety with a negative charge localized on N5O5 group and a positive charge on N(21)–C(2)–N(3)–C(4)–N(4) moiety. H_2**L1** and H_2**L2** protonations are accomplished by the vanishing of a typical absorption band at 525 nm, this corresponds to σ–π^* forbidden electronic transition of the non-bonding electronic pair of N atom of C5NO group. Thus, the vanishing of these bands proves the protonation of such N atom. The reactivity of H_2**L1** and H_2**L2** against Zn(II) fits well with the electronic structures of the ligands. Neutral H_2**L1** ligand forms a mononuclear [Zn(H_2**L1**)]$^{2+}$ complex in which the oxygen atom of C5NO group is used as weak donor base. On the other hand, in aqueous medium H**L1** and H**L2** anionic ligands act also as monofunctional ligands, using COO$^-$ as the donor weakly bonded group. These weak interactions just cause the existence of single mononuclear species in solution with a tendency to form polynuclear aggregates, as observed in other cases with this kind of ligands [5,7,8].

Otherwise, the solid structures of the two Zn(II) complexes reflect the versatility of these kinds of ligands. While $\{[Zn(H\mathbf{L1})_2]\cdot 2H_2O\}_n$ consists of 2D polynuclear aggregates with Zn(II) pentacoordinated to four differently coordinated H**L1** ligands, [Zn(H**L2**)$_2$(H_2O)$_4$] is a mononuclear complex with an octacoordinated Zn(II) ion to two equivalent COO$^-$-bonded H**L2** ligands and four water molecules.

3. Experimental

3.1. Synthesis

Ligand H_2**L1**, anhydrous *N*-2-(4-amino-1,6-dihydro-1-methyl-5-nitroso-6-oxopyrimidinyl)-L-valine, was prepared as previously described [2]. ^{1}H NMR (DMSO-d_6) δ (ppm): 10.83 (s, 1H), 8.31 (d, 1H), 7.68 (w, 1H), 4.48 (d, 1H), 2.21 (m, 1H), 0.96 (dd, 6H). ^{13}C NMR (DMSO-d_6) δ (ppm): 18.9, 19.0, 27.3, 30.3, 61.0, 141.6, 149.8, 154.1, 161.6, 174.6. ^{13}C NMR (H_2O, pH 6) δ (ppm): 21.2, 21.3, 30.1, 30.3, 32.8, 66.8, 143.5, 154.3, 157.4, 166.2, 180.7. ^{13}C NMR (H_2O, pH 12.2) δ (ppm): 20.7, 21.9, 29.04, 34.43, 70.82, 142.88, 160.2, 162.2, 170.8, 182.64.

3.2. N-2-(4-amino-1,6-dihydro-1-methyl-5-nitroso-6-oxopyrimidinyl)glycylglycine (H_2L2)

A solution of glycylglycine (2.11 g, 16 mmol) in aqueous KOH (16 ml, 1 mol dm^{-3}) was added to 4-amino-1,6-dihydro-1-methyl-2-methoxy-5-nitroso-6-oxopyrimidine monohydrate (3.23 g, 16 mmol) suspended in acetonitrile (50 ml). The mixture was then refluxed for 1.5 h and the resulting solution cooled at room temperature. At once it was acidified with 2 N HCl up to pH value of ca. 3 and then vacuum evaporated to give a crystalline solid. The product was washed with water, ethanol and diethylether and recrystallized in water. *Anal*. Calc. for $C_9N_6O_5H_{12}$: C, 38.03; H, 4.25; N, 29.57. Found: C, 37.81; H, 4.35; N, 28.97%. ^{1}H NMR (DMSO-d_6) δ (ppm): 12.58 (s, 1H), 10.90 (d, 1H), 8.37 (d, 1H), 8.33 (m, 2H), 4.04 (d, 2H), 3.75 (d, 2H), 3.37 (s, 3H). ^{13}C NMR (DMSO-d_6) δ (ppm): 27.4, 44.3, 110.1, 142.1, 149.7, 154.9, 161.6, 168.5, 171.1. ^{13}C NMR (H_2O, pH 6) δ (ppm): 30.4, 46.0, 47.5, 143.7, 154.2, 158.3, 166.3, 173.8, 179.2. ^{13}C NMR (H_2O, pH 12.3) δ (ppm): 31.0, 45.9, 51.5, 152.6, 154.7, 156.6, 167.0, 176.6, 179.3.

3.3. $\{[Zn(HL1)_2]\cdot 2H_2O\}_n$ (1)

$ZnCl_2\cdot H_2O$ (68.14 mg, 0.5 mmol) was added to a solution of H_2**L1** (134.5 mg, 0.5 mmol) and KOH (0.5 mmol) in water (25 ml), resulting in a solution of pH 5. Orange crystals of $\{[Zn(H\mathbf{L1})_2]\cdot 2H_2O\}_n$ suitable for X-ray analysis were obtained by slow evaporation at the air during 24 h. *Anal*. Calc. for $ZnC_{20}H_{32}N_{10}O_{10}$: C, 37.65; H, 5.02; N, 21.96. Found: C, 37.51; H, 5.08; N, 21.87%.

3.4. $[Zn(HL2)_2(H_2O)_4]$ (2)

$ZnCl_2\cdot H_2O$ (68.14 mg, 0.5 mmol) was added to a solution of H_2**L2** (142 mg, 0.5 mmol) and KOH (0.5 mmol) in water (50 ml). This solution (pH 4.2) was left to evaporate during three days at the air until formation of violet crystals. This solid keeps its crystalline appearance, whereas, is submerged in the mother liquor. In this way, it was mounted into a Lindeman tube for X-ray analysis. Otherwise, when this solid was filtered off it became partially dehydrated. *Anal*. Calc. for $ZnC_{18}H_{28}N_{12}O_{13}$: C, 31.60; H, 4.10; N, 24.59. Found: C, 31.86; H, 4.18; N, 24.23%.

3.5. X-ray structure analyses

Details for data collections and structure refinement are summarized in Table 4.

Table 4
Crystallographic data for $\{[Zn(HL1)_2]\cdot 2H_2O\}_n$ and $[Zn(HL2)_2(H_2O)_4]$

	$\{[Zn(HL1)_2]\cdot 2H_2O\}_n$	$[Zn(HL2)_2(H_2O)_4]$
Empirical formula	$C_{20}H_{32}N_{10}O_{10}Zn$	$C_{18}H_{30}N_{12}O_{14}Zn$
Formula weight	637.93	703.91
T (K)	293(2)	293(2)
Wavelength (Å)	0.71073	0.71073
Space group	$P2_1$	$P\bar{1}$
a (Å)	10.3670(9)	7.3450(7)
b (Å)	7.5199(8)	7.4785(7)
c (Å)	18.5409(12)	14.081(1)
α (°)	90.00	83.38(1)
β (°)	95.913(6)	77.11(1)
γ (°)	90.00	67.07(1)
V (Å^3)	1437.7(2)	694.1(1)
Z	2	1
d_{calc} (g cm^{-3})	1.474	1.684
μ (cm^{-1})	0.922	0.976
R^a	0.0409	0.0323
$R_w{}^b$	0.0911	0.0864

[a] $R = \sum(|F_o| - |F_c|)\sum|F_o|$.
[b] $R_w = \left[\left|\sum w(|F_o| - |F_c|)^2\right|\sum w|F_o|^2\right]^{1/2}$.

3.6. X-ray structure of $\{[Zn(HL1)_2]\cdot 2H_2O\}_n$

The unit cell parameters were determined and the data collected on a STOE STADI4 4 circle diffractometer at 293 K. The data were corrected for Lorentz-polarization effects and for dispersion, and an empirical absorption correction, using the program SHELXTL V.5 [9]. The structure was solved by direct methods and refined by using the SHELXTL V.5. All non-hydrogen atoms were refined anisotropically, while H-atoms were included in calculated positions and treated as riding atoms using the SHELXTL V.5 default parameters.

3.7. X-ray structure of $[Zn(HL2)_2(H_2O)_4]$

The unit cell parameters and the intensity data were collected at rt on a Stoe Image Plate Diffraction system using Mo Kα graphite monochromated radiation. Image plate distance 70 mm, ϕ oscillation scans 0°–200°, step $\Delta\phi = 1°$, θ range 2.97°–25.99°, d_{max}–d_{min} = 12.45–0.81 Å. The crystal was found to be a twin with ca. 15% overlapped reflections found on the 200 images. Only the reflections relating to the principal component of the twin were used for structure solution and refinement. The structure was solved by direct methods using the program SHELXS-97 [10]. The refinement and all further calculations were carried out using SHELXL-97 [10]. The H-atoms were located from difference Fourier maps and refined isotropically. The non-H atoms were refined anisotropically, using weighted full-matrix least-squares on F^2.

3.8. Potentiometric measurements

The equilibrium constants for H_2**L1** and H_2**L2** protonations and complexations were determined from emf data obtained from potentiometric measurements at 298.1 ± 0.1 K, by using the procedure previously described [11]. Ligands and metal concentration of (1–1.5)×10^{-3} mol dm^{-3} and 1:1 metal-to-ligand molar ratios were employed in the potentiometric measurements. Three titrations in each of the systems studied were performed with ca. 70 data point in each case. The HYPERQUAD [12] program was used in the calculation of the equilibrium constants from emf data.

3.9. Spectrophotometric measurements

Absorption spectra were recorded on a Perkin–Elmer Lambda 19 spectrophotometer. HCl and KOH water solutions were added to solutions containing H_2**L1** or H_2**L2** (0.1 M KCl) to adjust the pH values.

3.10. NMR spectroscopy

^{1}H (300.13 MHz) and ^{13}C (75.48 MHz) spectra in DMSO-d_6 and H_2O solutions (at different pH values) were recorded in a Bruker DPX300 spectrometer. To adjust the pH, small amounts of KOH were added to aqueous solutions of H_2**L1** and H_2**L2**.

4. Supplementary material

Crystallographic data (excluding structure factors) for the structural analysis have been deposited with the Cambridge Crystallographic Data Centre, CCDC Nos. 214666 for $\{[Zn(HL1)_2]\cdot 2H_2O\}_n$ and 214667 for $[Zn(HL2)_2(H_2O)_4]$. Copies of this information may be obtained free of charge from The Director, CCDC, 12 Union Road, Cambridge CB2 1EZ, UK (fax: +44-1223-336-033; e-mail: deposit@ccdc.cam.ac.uk or www: http://www.ccdc.cam.ac.uk).

Acknowledgements

Some of the authors are gratefully acknowledged for financial support by the Spanish Ministerio de Ciencia y Tecnología (Proyecto PPQ2000-1667) and by Junta de Andalucía (FQM-273).

References

[1] (a) M. Muthuraman, M. Bagieu-Beucher, R. Masse, J.-F. Nicoud, R.G. Desiraju, J. Mater. Chem. 9 (1999) 1471, and references therein;

(b) M. Muthuraman, J.-F. Nicoud, M. Bagieu-Beucher, Acta Crystallogr., Sect. C 56 (2000) 1077.
[2] J.N. Low, M. López, P. Arranz, J. Cobo, M.L. Godino, R. López, M.D. Gutiérrez, M. Melguizo, G. Ferguson, C. Glidewell, Acta Crystallogr., Sect. B 56 (2000) 882.
[3] J.N. Low, A. Quesada, C. Glidewell, M.A. Fontecha, P. Arranz, M.L. Godino, R. López, Acta Crystallogr., Sect. E 58 (2002) o942.
[4] P. Arranz-Mascarós, Ph.D. Thesis, University of Jaén, Spain, 1997.
[5] J.M. Moreno, P. Arranz-Mascarós, R. López-Garzón, M.D. Gutiérrez-Valero, M.L. Godino-Salido, J. Cobo-Domingo, Polyhedron 18 (1999) 1635.
[6] M.T. Beck, I. Nagypal, Chemistry of Complex Equilibria, Wiley, New York, 1990.
[7] (a) P. Arranz-Mascarós, M.L. Godino-Salido, R. López-Garzón, M.D. Gutiérrez-Valero, J.M. Moreno, Polyhedron 18 (1999) 793;
(b) P. Arranz-Mascarós, M.L. Godino-Salido, R. López-Garzón, M.D. Gutiérrez-Valero, J.M. Moreno, Polyhedron 18 (1999) 689;
(c) R. López-Garzón, P. Arranz-Mascarós, M.L. Godino-Salido, M.D. Gutiérrez-Valero, A. Pérez-Cadenas, J. Cobo-Domingo, J.M. Moreno, Inorg. Chim. Acta 308 (2000) 59;
(d) J.N. Low, J.M. Moreno, P. Arranz, M.L. Godino, R. López, J. Cobo, C. Glidewell, Acta Crystallogr., Sect. B 57 (2001) 317;
(e) J.N. Low, P. Arranz, J. Cobo, M.A. Fontecha, M.L. Godino, R. López, C. Glidewell, Acta Crystallogr., Sect. C 57 (2001) 534;
(f) J.N. Low, P. Arranz, J. Cobo, M.A. Fontecha, M.L. Godino, R. López, D. Cannon, C. Glidewell, Acta Crystallogr., Sect. C 57 (2001) 680.
[8] P. Arranz-Mascarós, R. López-Garzón, M.D. Gutiérrez-Valero, M.L. Godino-Salido, J.M. Moreno, Inorg. Chim. Acta 304 (2000) 137.
[9] SHELXTL PC, version 5.0, Siemens Analytical X.Ray Instruments, Madison, WI, 1995.
[10] G.M. Sheldrick, SHELXS-97: Program for the Solution of Crystal Structures; SHELXL-97: Program for the Refinement of Crystal Structures, University of Göttingen, Göttingen, Germany, 1997.
[11] M.L. Godino-Salido, M.D. Gutiérrez-Valero, R. López-Garzón, J.M. Moreno, Inorg. Chim. Acta 221 (1994) 127.
[12] P. Gans, A. Sabatini, A. Vacca, Talanta 43 (1996) 807.